Ground-based Laser Imaging for Assessing Three-dimensional Forest Canopy Structure

Jason G. Henning and Philip J. Radtke

Abstract

Improved understanding of the role of forests in carbon, nutrient, and water cycling can be facilitated with improved assessments of canopy structure, better linking leaf-level processes to canopy structure and forest growth. We examined the use of high-resolution, ground-based laser imaging for the spatially explicit assessment of forest canopies. Multiple range images were obtained and aligned during both leaf-off and leaf-on conditions on a 20 m × 40 m plot. The plot location was within a mixed species broadleaved deciduous forest in western North Carolina. Digital terrain and canopy height models were created for a 0.25 m square grid. Horizontal, vertical, and three-dimensional distributions of plant area index, created using gap-fraction based estimation, had 0.5 m resolution for a cubic lattice. Individual tree measurements, including tree positions and diameter at breast height, were made from the scanner data with positions, on average, within 0.43 m and diameters within 5 cm of independent measurements, respectively. Our methods and results confirm that applications of ground-based laser scanning provide high-resolution, spatially-explicit measures of plot-level forest canopy structure.

Introduction

Canopy structure, the amount and spatial distribution of aboveground vegetation, directly affects light availability in forests (Parent and Messier, 1996). As a result, this structure impacts the ability of different species and individual trees to reproduce, survive and grow (Canham *et al*., 1994; Brunner, 1998; Gratzer *et al*., 2004). A significant limitation to understanding the relationships between plant structure and function is the lack of spatially explicit data at scales useful for determining linkages between canopy level processes and individual tree growth and mortality (Parker *et al*., 2004). Many existing models that quantify relationships between canopy structure and function rely on generalized canopy representations such as cones, cylinders, or cubes of uniform foliage density (Aber and Federer, 1992; Dai, 1996; Brunner and Nigh, 2000; Kussner and Mosandl, 2000; MacFarlane *et al*., 2002; Gratzer *et al*., 2004; Rhoads *et al*., 2004). Detailed information on the spatial distribution of canopy surfaces would facilitate increased understanding of how light transmittance and interception affect tree processes including growth, transpiration, respiration and allocation of carbon and nutrients (Canham *et al*., 1994; MacFarlane *et al*., 2003; Gratzer *et al*., 2004). Research has determined the importance of the spatial distribution of branches, foliage, and small light pathways in light capture and forest growth (Canham *et al*., 1990; Chazdon and Pearcy, 1991).

Most existing methods for quantifying canopy structure are limited in their capacity to make detailed, spatially explicit measurements. For example, indirect measurement tools provide one- or two-dimensional summaries of canopy structure observable from a single viewpoint or averaged over an area of forest (Parent and Messier, 1996; Comeau *et al*., 1998; Gendron *et al*., 1998; Kussner and Mosandl, 2000). Direct or semi-direct measurement techniques, such as leaf-litter collection, stratified clipping, or point-quadrat sampling may be labor intensive or destructive and are not always entirely spatially explicit in three-dimensions (3D) (Warren Wilson, 1959; Ford and Newbould, 1971; Kussner and Mosandl, 2000; Bréda, 2003). In contrast, ground-based laser scanning provides non-destructive, high-resolution, 3D surveys of canopy surfaces, which may address some of the challenges not met by existing techniques for measuring canopy structure (Lovell *et al*., 2003).

Applications of close-range, ground-based laser scanning technology are becoming increasingly common in fields such as surveying, architecture, heritage preservation, engineering, and industrial processing where interest lies in detailed 3D characterization of natural and engineered surfaces (Besl and McKay, 1992; Fitzgibbon *et al*., 1997; Zhilkin and Alexander, 2000; Hetzel *et al*., 2001). A ground-based laser scanner is a type of light detection and ranging (lidar) system that operates from a stationary terrestrial platform. Airborne lidar systems, widely employed in forestry applications, have proven useful for landscape-level characterizations, (Nelson *et al*., 1988; Lefsky *et al*., 1999; Harding *et al*., 2001; Drake *et al*., 2002; Zimble *et al*., 2003). However, airborne systems, with minimum footprint sizes of 0.1 m and 0.25 m between pulses and limited incidence angles may not be useful for detecting small canopy elements (Parker *et al*., 2004; Tickle *et al*., 2006). Additionally, single- or multiple-pulse, handheld or backpack-mounted laser range finders have been employed in a few upward looking ground-based applications (Radtke and Bolstad, 2001; Parker *et al*., 2004). The accuracy of data collected with these tools is often limited by the ability of the user to direct the range finder in a precisely known direction.

Recently, a small number of exploratory studies employing ground-based laser scanners for forest measurements have been reported. Some studies used data from several range images to make individual tree measurements or plot-level summaries (Hopkinson *et al*., 2004; Pfeifer *et al*., 2004; Thies *et al*., 2004; Henning, 2005; Watt and Donoghue, 2005). Other studies made canopy measurements from single range images captured with scanning systems (Tanaka *et al*.,

Jason G. Henning was with the Virginia Tech, Department of Forestry and is currently with the University of New Hampshire, Department of Natural Resources, 215 James Hall, Durham, NH 03824 (jason.henning@unh.edu.)

Philip J. Radtke is with the Virginia Tech, Department of Forestry, 315 Cheatham Hall, Blacksburg, VA 24061(pradtke@vt.edu).

Photogrammetric Engineering & Remote Sensing
Vol. 72, No. 12, December 2006, pp. 1349–1358.

0099-1112/06/7212–1349/$3.00/0

1998; Lovell *et al.*, 2003; Tanaka *et al.*, 2004). To date, applications exploring the use of scans acquired from multiple viewpoints to assess the spatial distribution of canopy structure are rare (Chasmer *et al.*, 2004).

Ground-based laser scanning data can provide a variety of canopy characterizations at fine scales and high resolutions. Ground-based laser scanning holds particular appeal for providing measurements necessary to quantify relationships between canopy function and structure. However, before this tool can be widely applied, methods for summarizing the data and extracting features of interest need to be developed.

The research presented here used range images obtained from multiple viewpoints on a forested plot to generate multidimensional characterizations of forest canopy structure. Methods to combine range images from multiple viewpoints and create useful summaries of forest canopy structure were developed to facilitate the use of ground-based laser scanning for this application. Characterizations of interest included (a) 2D and 3D summaries of leaf-area and plant-area indices, (b) individual tree parameters such as height, location, and diameter, and (c) digital terrain and canopy height models. Specific goals included quantifying differences in characterizations obtained under leaf-off and leaf-on canopy conditions, and comparing scanner-derived estimates to independent measurements.

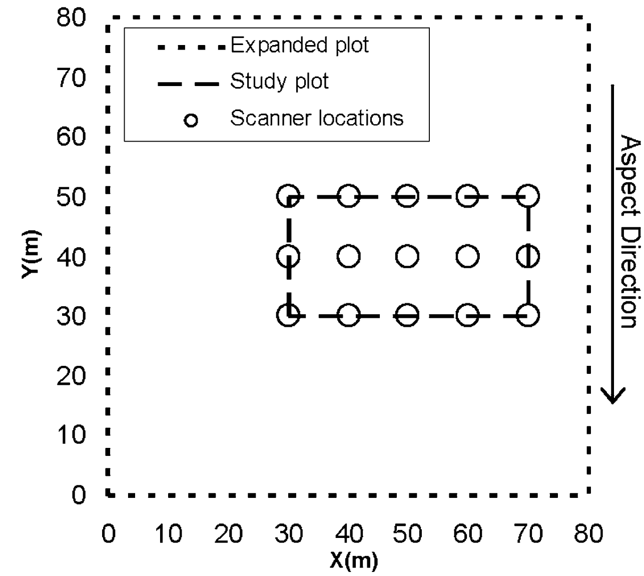

Figure 1. Plot layout of terrestrial gradient plot 218, with scanner positions. Plot axes were defined relative to slope aspect.

Methods

Data

All data were collected at the U.S. Forest Service Coweeta Hydrologic Laboratory (35° 03′ N, 83° 26′ W) in the southern Appalachian Mountains of western North Carolina. The site was chosen to make use of existing data collections in testing the accuracy of scanner-derived measurements. A number of detailed vegetation measurements were available from the archived data set maintained as part of the National Science Foundation sponsored Long Term Ecological Research (LTER) Network. Two data sources were used in this research. The first source was the set of archived data collected during past and ongoing ecological research at the study site (see http://coweeta.ecology.uga.edu). The second source was sets of range images captured with a ground-based laser scanner.

Laser data were collected at a permanent plot denoted as terrestrial gradient plot 2, watershed 18, i.e., "plot 218," one of five plots in a terrestrial gradient tree growth study at Coweeta. Although some long-term field measurements were available over an 80 m × 80 m area at plot 218, the primary interest here was an interior 20 m × 40 m study plot (Figure 1). The LTER tree growth survey database included records of tree species, diameters at breast height (DBH, recorded in cm at 1.37 m above ground) and positions recorded in Cartesian coordinates (m) from *X*- and *Y*-axes defined as the plot borders shown in Figure 1. The growth survey data were obtained from the Coweeta LTER website (http://coweeta. ecology.uga.edu). From the available data we acquired the positions and DBH of all trees on the study plot with DBH ≥10 cm surveyed in 2002.

Range images of the study plot were obtained during periods of leaf-off (18 December 2001) and leaf-on (21 August 2002), using a tripod-mounted, model LMS-Z210, motorized 3D laser-imaging sensor, distributed by Riegl USA, Inc. The LMS-Z210 operates on the time-of-flight principle and uses a mirror rotated about two axes to direct laser pulses at known angles (Figure 2). Range images were obtained from 15 positions corresponding to the nodes of a 10 m × 10 m grid covering the study plot (Figure 1). Node positions corresponded to monumented grid corners installed as part of the terrestrial gradient study.

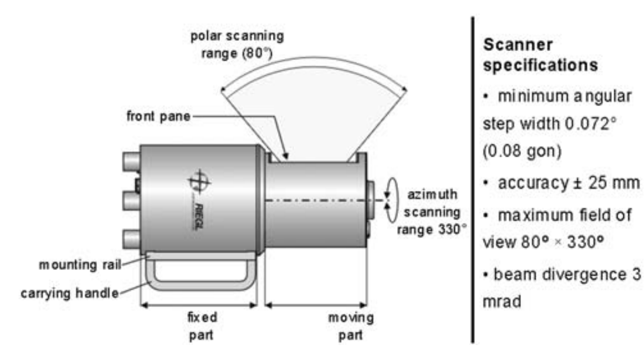

Figure 2. Schematic diagram and hardware specifications of the LMS-Z210 ground-based laser scanner. Scanner pictured in prone position as used in this research. (Image courtesy of RIEGL Laser Measurement Systems; www.riegl.com).

Range image fields of view were set to fully cover the (20 m × 40 m) plot and minimize off-plot coverage, reducing the time needed for image acquisition. Initially overhead scans were obtained using the scanner's maximum field of view (80° × 330° or 1.40 × 5.76 rad) with an angular step width of 0.18° (0.0031 rad). Given this field of view (Figure 2), it was possible to sample an angle 80° wide through a zenith angle of 0° to ±165°. The 80° limit generally required the acquisition of three images at each node to ensure complete sampling of the canopy above the study plot. However, only 41 scans were obtained for the leaf-off data set with only two scans acquired at the each of the four corner nodes. It was possible to maintain complete coverage of the plot using only two scans at the corner nodes, but little was gained in the efficiency of data collection or processing, so the leaf-on data were collected using three scans at all nodes for a total of 45 leaf-on scans. Increased efficiency was obtained for the leaf-on scans by only scanning through a zenith angle of 0° to ±135°; minimizing time spent scanning the ground close to the scanner.

Registration

A series of registration procedures were carried out to align all images to the study plot coordinate system. Registration employed control points from common stem surfaces visible in multiple range images using the method of Henning and Radtke (2006). In general, the method involved extracting successive thin horizontal slices of points representing tree boles, filtering noise points related to branches and irregular stem surfaces, and determining the X and Y coordinates of a slice's center as the point resulting in the minimum standard deviation of the distance from each filtered point to the stem center. This method resulted in a vector of points representing the pith of the selected tree. Henning and Radtke (2006) reported accuracies in diameter estimation <1 cm below the base of the live crown. They employed angular step widths as small as 0.06° and focused on clearly visible trees typically within 5 m of the scanner.

Alignments of scans were performed in a pair-wise manner using a 3 × 3 rotation matrix denoted $\mathbf{A}$ and a translation 3-vector denoted $\tilde{\mathbf{b}}$. The X, Y, and Z coordinates of any point, denoted by the 3-vector $\tilde{\mathbf{p}}$, were transformed from one range image to its corresponding location in a target coordinate system by:

$$T(\tilde{\mathbf{p}}) = \mathbf{A}\tilde{\mathbf{p}} + \tilde{\mathbf{b}} \qquad (1)$$

The positions and angular orientations of the scanner in the field had been recorded, allowing for an approximation of initial $\mathbf{A}$ and $\tilde{\mathbf{b}}$ parameters that served to coarsely align each image to the study plot X-Y coordinate system. Following this coarse alignment, scan pairs or triplets from a common node were co-registered, in a step referred to as "within-node" registration. Next, "between-node" registrations aligned range images acquired from one plot node to those acquired at another node. Image alignment also incorporated ground surfaces to reduce registration errors in the vertical (Z) direction. A final transformation ensured that scanner locations were optimally matched to their corresponding positions in the study plot X-Y coordinate system.

For each alignment, $\mathbf{A}$ and $\tilde{\mathbf{b}}$ transformation parameters were estimated using Besl and McKay's (1992) iterative closest point (ICP) algorithm. The ICP algorithm was applied to extracted sets of common surfaces from range images being registered. For within-node registrations tree stem surfaces were used. For between-node registrations common stem surfaces were not generally visible or easily matched between images; so, stem centers were used as registration control points. Through the application of a series of estimated $\mathbf{A}$ and $\tilde{\mathbf{b}}$ transformations, all 41 leaf-off images were aligned to the plot coordinate system. The 45 leaf-on images were similarly aligned to the plot coordinate system. We refer to these data sets as the aligned point clouds for leaf-off and leaf-on conditions, respectively.

Distribution of Plant Area Index and Leaf Area Index

In broad leaf canopies leaf area index (LAI) has been defined as the one-sided area of leaves per unit of ground area. Alternatively, plant area index (PAI) includes all plant material and can be considered one half of the total area of all plant surfaces per unit of ground area. To create spatially explicit representations of canopy structure, PAI was estimated for cubic volumes or voxels in a regular lattice covering the volume above the plot (Chasmer *et al.*, 2004). Leaf-off and leaf-on PAI for each voxel were estimated from aligned point clouds using the method of MacArthur and Horn (1969),

$$\mathrm{PAI_i} = -ln(\mathrm{P_i}/(\mathrm{P_i} + \mathrm{I_i})) \qquad (2)$$

where $\mathrm{P_i}$ is the number of pulses passing through voxel i and $\mathrm{I_i}$ is the number of pulses intercepted within voxel i. A voxel size of 0.5 m on a side ensured that the majority of the voxels were sampled by a minimum number of laser pulses. Voxels completely above the canopy top or within 0.5 m of the ground were ignored. The horizontal PAI distribution for the plot was calculated by summing the PAI in the column of voxels above each 0.5 m × 0.5 m horizontal cell. Vertical PAI profiles resulted from averaging the PAI values within vertical 0.5 m bins from the ground to the top of the canopy. Estimates of LAI were obtained by taking the difference between leaf-on and leaf-off PAI.

Tree Heights, Positions, and DBH

Tree heights and the positions of selected tree tops were estimated manually by inspection and cropping of 3D scatter plots. Heights were estimated by visually locating the base and top of a tree in a scatter plot and calculating the vertical distance between those points. These manual height estimates were made from each image in which a tree was fully visible and averaged.

Maps of stem position and DBH were created from tree stem sections extracted from range images. We extracted potential stem sections from each image using an automated algorithm and verified that these extracted point sets corresponded to trees using graphical inspection (Henning, 2005). From cross-sections of the stem section point clouds at breast height we calculated DBH and stem X and Y-positions using estimated stem centers. Finally, because a single tree could be present in more than one image, DBH estimates and positions for a stem were averaged across all the images in which the corresponding tree appeared.

Digital Terrain Model and Canopy Height Model

Digital terrain models (DTMs) were created by finding the minimum height of the laser returns falling within each horizontal cell in a square grid covering the plot, followed by a filtering out of heights not representing ground surfaces (Axelsson, 1999; Henning, 2005). A cell size of 0.25 m × 0.25 m was used resulting in a plot tessellation of 12,800 grid cells.

Canopy top surface models (CTSMs) and canopy height models (CHMs) were also created for the study plot using 0.25 m × 0.25 m cells. The CTSM corresponded to the maximum height of the laser returns within the horizontal boundaries of each cell. No filtering of points was performed for the CTSM. The CHM was computed by subtracting DTM height values from the height values of corresponding cells in the CTSM (Popescu *et al.*, 2002). Two DTMs, CTSMs, and CHMs were created, one from the set of leaf-off scans, and another from the set of leaf-on scans.

Results

Some general differences between leaf-off and leaf-on conditions were noted from direct observations of range images (Plate 1). It was noted that the volume of the canopy blocked from the scanner's viewpoint in range images was lower in leaf-off scans than in corresponding leaf-on scans. Evidence for this included the appearance of larger and more frequent canopy gaps in leaf-off images (Plate 1a). Also, foliage near the scanner was readily visible in leaf-on images that did not appear in leaf-off images (Plate 1b). The leaf-off range image in Plate 1a included 13,927 non-intercepted pulses, represented by black pixels. In contrast the leaf-on image (Plate 1b) had only 994 non-intercepted pulses. Similar differences were noted in comparisons of other range images obtained under leaf-off and leaf-on conditions. The distribution of measured ranges in leaf-off images included

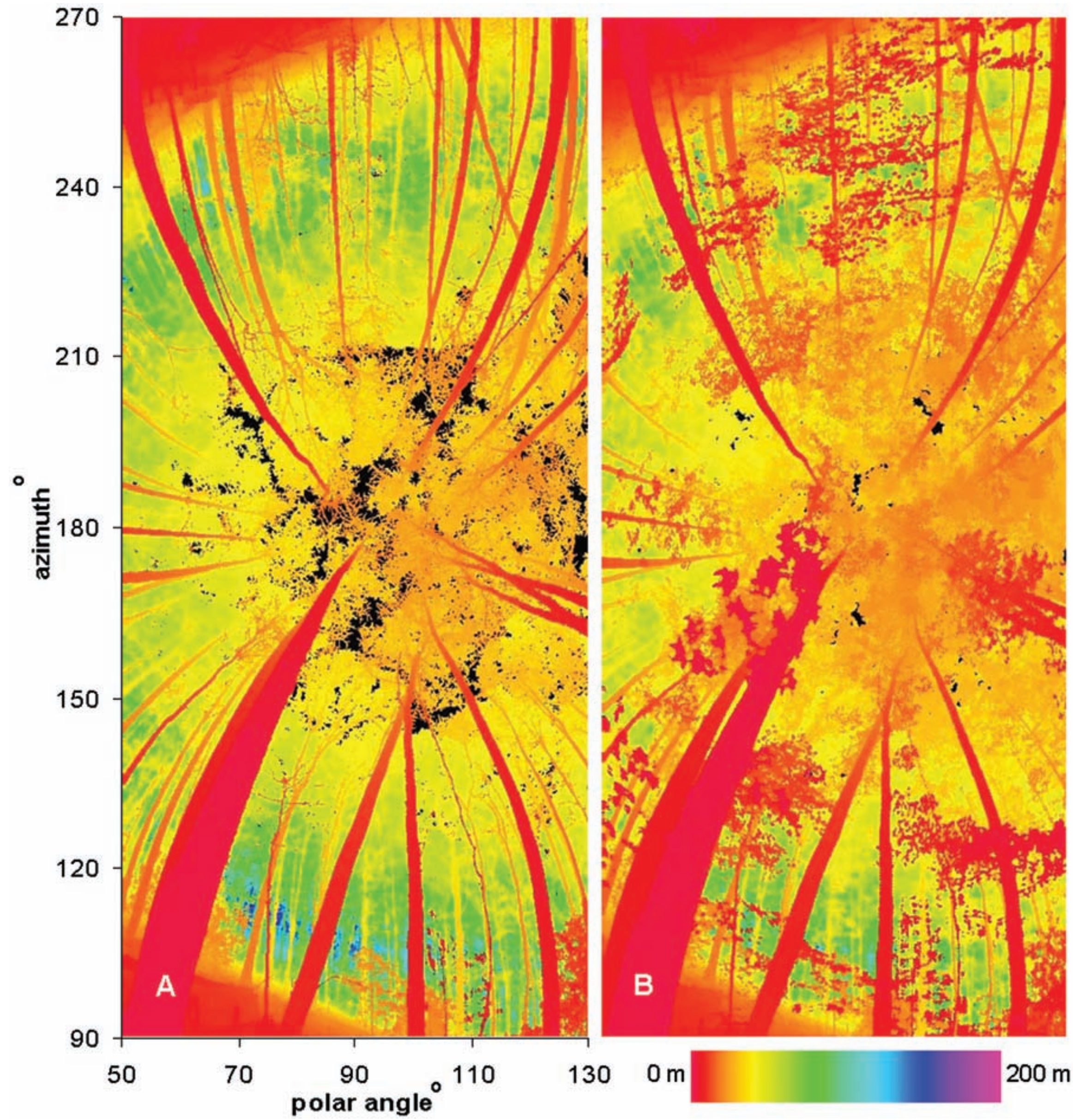

Plate 1. False color range images generated by the scanner positioned at (60 m, 40 m) on the study plot (Figure 1), during leaf-off (a) and leaf-on (b). The images have an angular step width of 0.18° and represent a truncated 80° × 180° field of view centered on the zenith. Black pixels indicate no return of laser pulse.

measurements that penetrated farther into the forest than those in leaf-on images. For example, the average range value in the leaf-off image (Plate 1a) was 32.6 m while the average range measurement in the leaf-on image (Plate 1b) was 25.2 m.

Rotating 3D scatter plots were examined to manually identify individual trees in point clouds, and to facilitate inspection of aligned point clouds from multiple range images. The 3D scatter plots provided additional characterizations of relative abundances in plant area for leaf-off and leaf-on conditions (Figure 3). The data shown in Figure 3 consist of 92,913 and 157,592 points from the leaf-off and leaf-on conditions, respectively. The alignment of point clouds was verified by examining distinctly visible trees, such as a 33.4 cm DBH *Carya glabra* (Mill.) tree identified by the arrow in Figure 3. The lower 3 m section of the tree trunk was not entirely visible in the leaf-on scans because that portion of the tree was occluded by understory foliage from some scanner viewpoints (Figure 3b).

Distribution of PAI and LAI

Voxelization resulted in a total of 217,967 voxels, each with a volume of 0.125 m^3, characterizing the plot volume during leaf-off conditions. A slightly larger canopy volume consisting of 218,170 voxels was scanned during leaf-on conditions. The difference in the number of voxels reflects minor differences in the height of the canopy assessed during leaf-on and leaf-off. The height of maximum PAI was similar for leaf-off and leaf-on at 34.5 m and 34 m, respectively (Figure 4). The heights of the largest differences between leaf-on and leaf-off PAI correspond to the heights where we expect the most foliage was displayed during leaf-on conditions (Figure 4). Some PAI differences were noted near ground level, but the majority occurred higher in

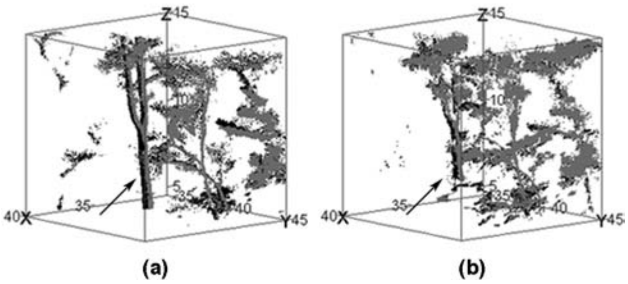

Figure 3. Three-dimensional scatter plot of a 10 m × 10 m × 10 m canopy volume assessed during leaf-off (a) and leaf-on (b). Gray points indicate data captured from plot node (30 m, 40 m). Black points indicate data captured from node (40 m, 40 m). Volume pictured was centered at (35 m, 40 m, 10 m) relative to the study plot (Figure 1).

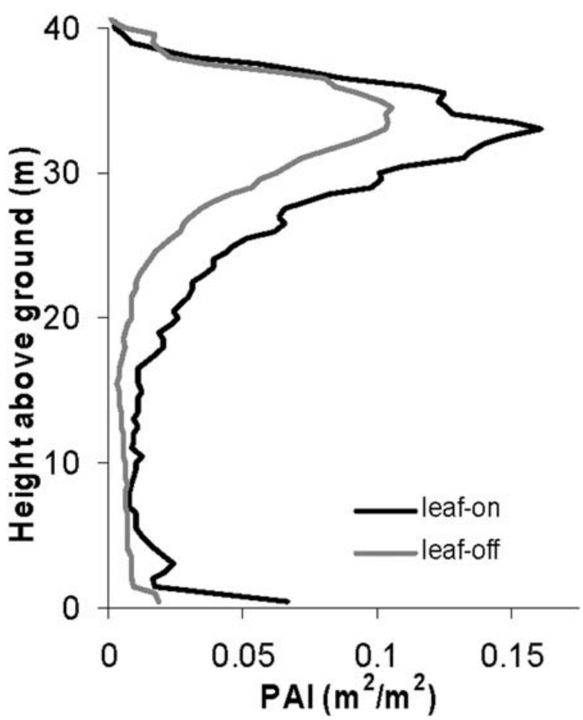

Figure 4. The mean vertical distribution of PAI over the entire plot, estimated using a 0.5 m voxel size, from leaf-off and leaf-on scanner data.

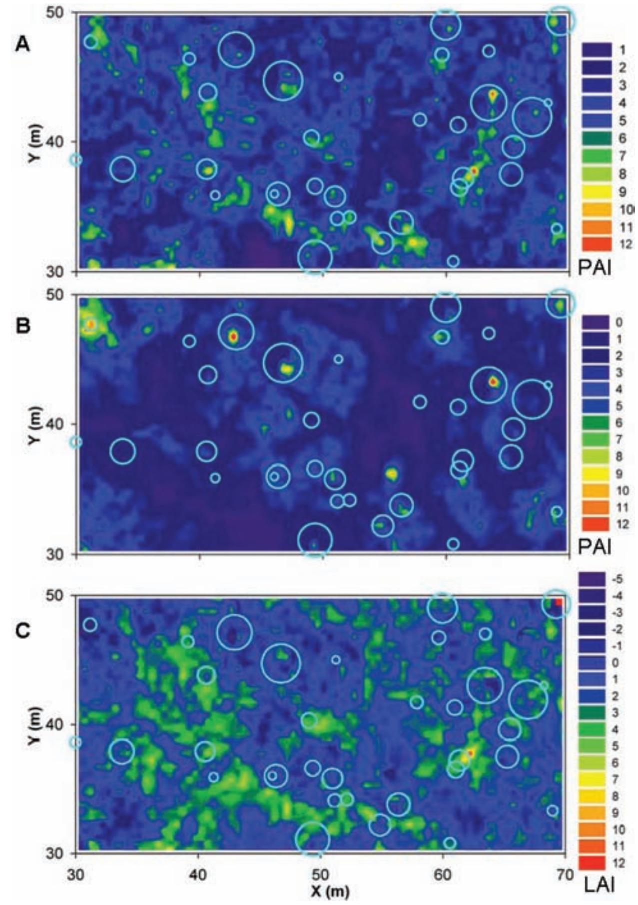

Plate 2. Horizontal PAI distribution from leaf-on (a) and leaf-off (b) scanner data using the 0.5 m voxel size. An approximate LAI distribution (c) was created by subtracting (b) from (a). Circles represent locations of tress with DBH ≥10 cm measured during the 2002 Coweeta tree growth survey and are proportional to tree DBH.

the canopy. The largest differences between leaf-on and leaf-off PAI occurred from 20 m to 35 m above ground.

Variability in the horizontal distribution of PAI was characterized with the ground-based laser scanner (Plate 2). The average leaf-on PAI, estimated by averaging PAI across the 3,200 cells (Plate 2a), was 3.5 m^2/m^2 with a standard deviation of 1.5 m^2/m^2. The average plot-level leaf-off PAI was 2.1 m^2/m^2 with a standard deviation of 1.5 m^2/m^2. The highest concentrations of PAI generally corresponded to the locations of trees recorded in the tree growth survey (Plate 2). Similar variability was seen in the horizontal distribution of LAI (Plate 2c) estimated by subtracting the leaf-off PAI estimates from the leaf-on estimates. The average LAI estimated for the plot was 1.4 m^2/m^2 with a standard deviation of 1.8 m^2/m^2. Approximately 20 percent of the cells had negative LAI values (Plate 2c).

Tree Heights, Positions, and DBH

Scanner-derived stem maps located trees, on average, within 0.43 m of their position recorded in the tree growth survey stem maps. For some trees, DBH estimates from the scanner data were higher than corresponding field measured DBH (Plate 3 and Table 1). Typically, the largest errors in estimated DBH were made on the thinnest trees, especially on trees with field-measured DBH values of approximately 10 cm. Ignoring the two trees with the smallest field-measured DBH, mean bias in DBH for leaf-off scans decreased to 0.018 m, and root mean square error decreased to 0.089 m from 0.048 m and 0.226 m, respectively, when all trees were included (Table 1). In general, scanner-derived stem maps exhibited better agreement with each other than with the growth survey stem map (Table 1, Plate 3).

Independent measurements of tree heights were not available for validation of scanner derived tree heights; however, height estimates were evaluated for consistency

TABLE 1. THE TOP TWO ROWS REPRESENT DIFFERENCES BETWEEN FIELD MEASUREMENTS FROM THE TREE GROWTH SURVEY AND VALUES ESTIMATED FROM SCANS OBTAINED UNDER LEAF-OFF AND LEAF-ON, RESPECTIVELY. THE BOTTOM ROW REPRESENTS DIFFERENCES BETWEEN LEAF-ON AND LEAF-OFF ESTIMATES FOR THE REPORTED NUMBER OF COMMON STEMS

Scan Acquisition	Number of Stems	Mean Position Error (m)	Standard Deviation of Position Errors (m)	Mean Bias in DBH (m)	Root Mean Square DBH Error (m)
Leaf-off	28	0.43	0.348	0.048	0.226
Leaf-on	22	0.39	0.231	0.047	0.204
Comparison of leaf-on and leaf-off	22	0.29	0.125	0.030	0.169

across scans and a height diameter relationship for scanner measurements was compared to an analogous relationship from an independent data set. Manual inspections of point clouds were used to estimate heights for a total of 20 trees, with eight having heights estimated from one range image, eight having heights estimated from two range images and four having heights estimated from three range images. For trees with heights estimated from multiple range images the average difference between the highest and lowest height estimate was 1.2 m with maximum and minimum absolute differences of 2.9 m and 0.1 m, respectively. A height diameter relationship,

$$ln(\text{Height}) = b_0 + b_1 \text{dbh}^{-1} \tag{3}$$

was fitted, using ordinary least squares optimization, to the scanner derived heights and the tree growth survey measured diameters (Avery and Burkhart, 2002). This relationship was also fit to unpublished data collected for *Liriodendron tulipifera* (L.) at the Coweeta Hydrologic Laboratory during the study described in Martin *et al*. (1998). The b_0 and b_1 parameters from the scanner data were 3.88 and −14.00 with standard errors of 0.06 and 1.6, respectively (Figure 5). Similarly, b_0 and b_1 parameters from the *L. tulipifera* data were 3.83 and −15.73 with standard errors of 0.14 and 3.14, respectively (Figure 5).

DTM and CHM

Graphical representation of the CHMs, DTMs and CTSMs generated from the sets of leaf-off and leaf-on scans were produced (Figure 6). The models shown in Figure 6 each consist of 12,800, 0.25 m × 0.25 m, cells. Differences in estimated heights for common cells facilitated comparison of leaf-off and leaf-on models. A difference value, d_{xy}, computed as,

$$d_{xy} = Z_{xy(\text{leaf-on})} - Z_{xy(\text{leaf-off})} \tag{4}$$

where $Z_{xy(\text{leaf-on})}$ and $Z_{xy(\text{leaf-off})}$ were the estimated *Z*s from cells at location *X-Y* in a DTM, CTSM, or CHM from the leaf-on and leaf-off range images, respectively.

Leaf-off and leaf-on CHMs were generally consistent (Table 2), but a small number of cells exhibited height estimates that were not in agreement. The consistency between the two models resulted in a median d_{xy} value of −0.30 m. The standard deviation of d_{xy} was 2.7 m. Observed d_{xy} values ranged from −17.8 m to 35.5 m. The extreme values of d_{xy} were observed in areas where canopy height changed rapidly, such as near the canopy gap at study plot

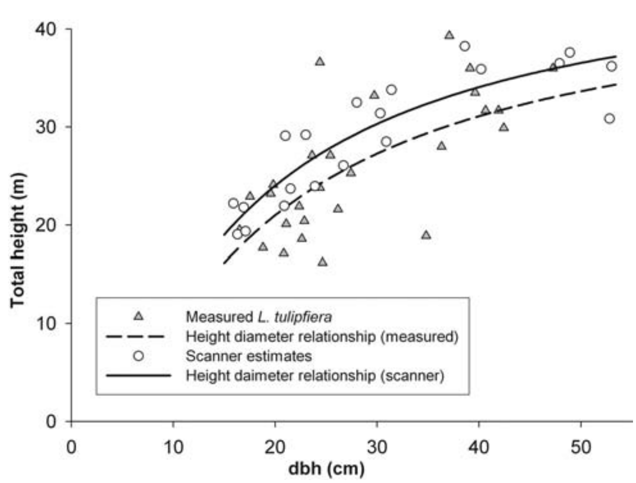

Figure 5. Scatter plots of scanner-derived heights and 2002 Coweeta tree growth survey DBH measurements as well as independent height and diameter measurements for *Liriodendron tulipifera* (L.). Trend lines correspond to Equation 3 fitted using ordinary least square optimization.

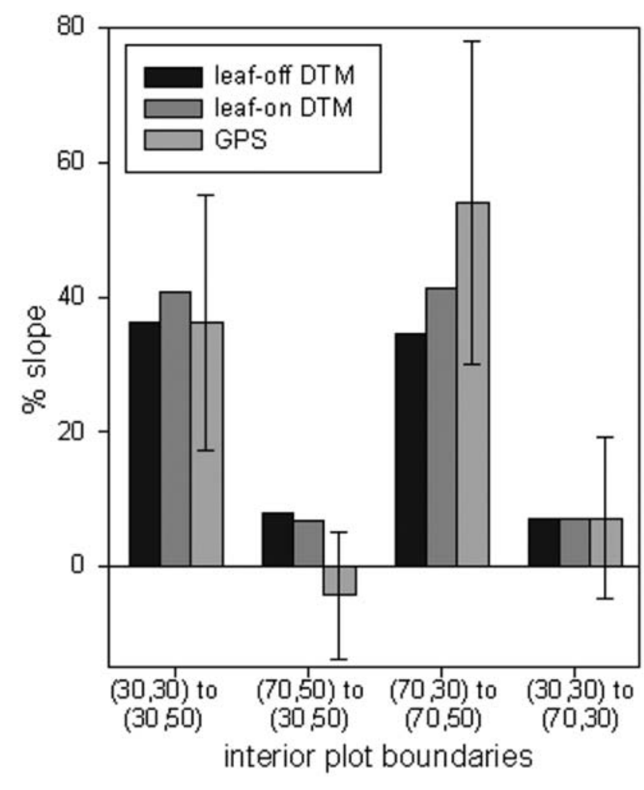

Figure 6. Comparison of ground surface slopes obtained using the corners of the leaf-off digital terrain model (DTM), leaf-on DTM and on-site GPS measurements. The error bars nominally represent ±1 standard deviation in the vertical direction.

Table 2. Summary Statistics for Leaf-on and Leaf-off Canopy Height Models (chms)

	Leaf-on chm	Leaf-off chm
Maximum ht (m)	41.9	41.8
Minimum ht (m)	8.4	0.7
Mean ht (m)	34.0	34.1
Standard Deviation of ht (m)	3.0	3.4

coordinates (45 m, 30 m) (Figure 7). The cells where leaf-off canopy height appeared to be much higher than leaf-on canopy height and the concentration of these cells near regions of rapid change in canopy height indicated that some registration of leaf-off to leaf-on scans may be warranted.

The ground slope of the study plot borders in the scanner-derived DTM generally agreed with the slope of the plot borders calculated from locations of the plot corners obtained by GPS (Figure 6). The GPS data were obtained from the Coweeta LTER website (http://coweeta.ecology.uga.edu). Three of the four slopes from the DTMs were within one weighted standard deviation of the slopes obtained using the GPS measurements (Figure 6).

Discussion and Conclusions

Ground-based laser scanning is emerging as a tool for forest canopy assessment. Many of the algorithms for registering, segmenting and analyzing the data were developed for engineering and surveying applications. As such, there are a number of practical considerations in adapting data and algorithms typically used for assessing uniform, geometric surfaces to the relatively small, variable and irregular surfaces common in natural, forested scenes (Gorte and Pfeifer, 2004; Henning and Radtke, 2006). Scanner applications often use targets placed within the scene or make use of the geometry of corners, edges, or other distinguishable features of scanned surfaces to determine registration control points (Besl and McKay, 1992; Watt and Donoghue, 2005). Other studies have reported concerns over the practicality of using artificial control targets in forested environments (Aschoff *et al.*, 2004; Pfeifer *et al.*, 2004). Here, registration control points were determined using tree surfaces, estimated stem

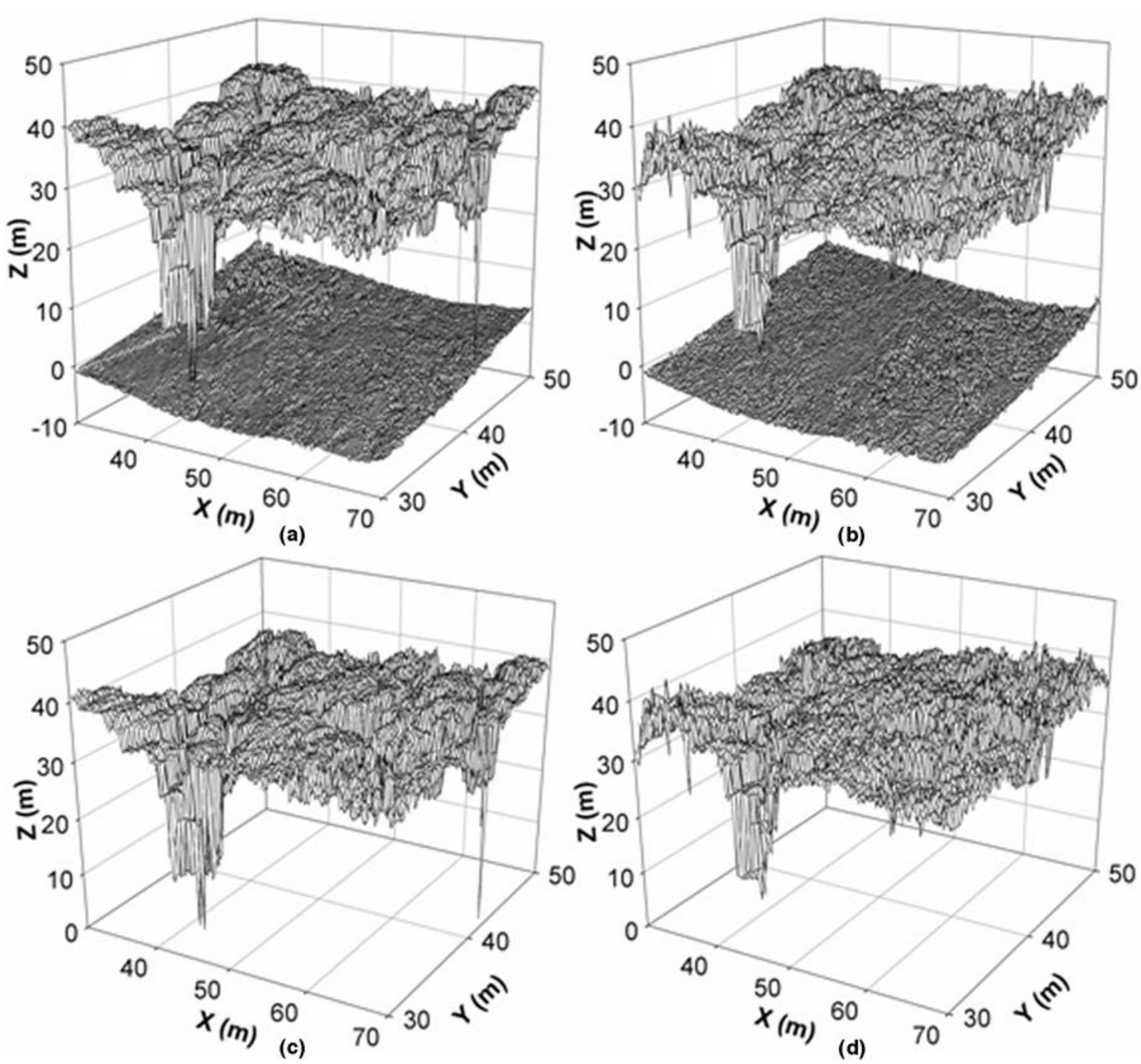

Figure 7. Digital terrain and canopy top surface models for the study plot from leaf-off (a) and leaf-on (b) scanner data. Canopy height models for the study plot from leaf-off (c) and leaf-on (d) scanner data.

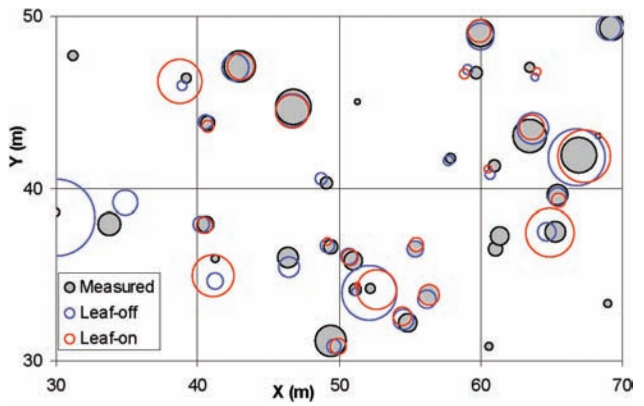

Plate 3. Stem maps of selected trees from the leaf-off and leaf-on scanner data. All trees measured in the 2002 Coweeta tree growth survey, with DBH ≥10 cm, are also shown.

centers, and ground surfaces. Registration using tree surfaces and stem centers has several advantages in natural scenes where it may be difficult to place targets that can be seen from multiple viewpoints (Gorte and Pfeifer, 2004; Henning and Radtke, 2006). First, the large number of potential control surfaces provides flexibility in the selection of control points so that the registration can be focused to create the best alignment for features of interest (Aschoff *et al*., 2004). Second, the upright nature of tree stems facilitates accurate registration high in the canopy, where measurements from laser scanning are likely to be of interest (Pfeifer *et al*., 2004).

In this and other research performed using ground-based laser scanning the data were typically used to develop canopy structure characterizations similar to existing canopy profiling methods (e.g., MacArthur and Horn, 1969; Aber and Federer, 1992; Radtke and Bolstad, 2001) often ignoring the 3D nature of the data (Figure 4 and Plate 2) (Lovell *et al*., 2003; Chasmer *et al*., 2004; Henning, 2005). Some methods are being developed to summarize range images of forested scenes by automated "skeletonization," or summarizing of the data that correspond to individual trees and their associated branches (Gorte and Winterhalder, 2004; Pfeifer *et al*., 2004). Collections of relative positions of skeletonized trees and branches in 3D may provide a more complete data source for examining canopy structure and its relationship to individual tree growth. The development of automated and objective forest canopy characterization techniques that exploit the resolution, scale and 3D nature of laser scanner data requires continuing research.

Vertical, horizontal, and 3D distributions of PAI and LAI provide appealing methods to relate ground-based laser scanning data to existing research and models, but validation of these characterizations is currently incomplete. Here the LAI estimates of 1.4 (m^2/m^2) were unrealistic given the results of Bolstad *et al*. (2001), who used leaf-litter collected over a two year period to estimate LAI ranging from 2.7 to 8.2, with an average of 5.8, for 16 sites across the Coweeta Hydrologic Laboratory. Following the methods of Parker *et al*. (2004) and Radtke and Bolstad (2001), we applied the transformation described by MacArthur and Horn (1969) to adjust for decreasing sampling rates due to occlusion of pulses further from the laser instrument. This method may have introduced biases, as it did not account for foliage inclination or non-vertical laser measurements (Warren Wilson, 1963). Another assumption of the estimation was that foliage was distributed randomly within voxels (Chen *et al*., 1991; van Gardingen *et al*., 1999). These assumptions were not evaluated here; however, characteristics of laser scanner data may make it possible to evaluate such assumptions in the future. For instance, since images from multiple viewpoints contributed to the estimated PAI of each cubic volume it may be possible to determine mean leaf angles and correct estimates accordingly (Warren Wilson, 1963). Additionally, Chasmer *et al*. (2004) were able to create profiles of the frequency of intercepted pulse returns directly from ground-based laser scanning data, ignoring changes in sampling rates, which may provide similar information to estimated LAI and PAI profiles.

Instrument-related biases such as beam divergence, return recording thresholds, registration accuracy, and beam inclination will also require consideration in the continued development of PAI and LAI estimation using ground-based ranging instruments (Lovell *et al*., 2003; Parker *et al*., 2004). In addressing biases in estimates of LAI and PAI, spatially explicit validation data will be needed. Distributions of PAI and LAI (Figure 4 and Plate 2) provide intuitively appealing results, but direct evaluation of their accuracy may require comparison to data gathered with labor intensive destructive sampling (Tanaka *et al*., 2004).

Here and elsewhere it has been possible to directly assess the accuracy of individual tree measurements made with a ground-based laser scanner. We observed mean position errors of 0.39 m and DBH errors of 4.7 cm using the leaf-on scanner data. We did not directly validate our height measurements, but noted that estimated height-diameter relationships were similar to those obtained using independent data (Figure 5). Hopkinson *et al*. (2004) manually extracted trees from five range images at two different plots and reported mean diameter errors near 1 cm for all trees and mean positional errors greater than 1.5 m. Thies and Spiecker (2004) determined tree positions automatically from registered range images and reported laser scanner-derived DBH estimates within 1.3 percent of measured values. A few studies have focused directly on making measurements of individual trees. Typically, these studies were able to determine tree parameters to a high degree of accuracy (Thies *et al*., 2004; Henning and Radtke, 2006). The arrangement of scanner viewpoints for plot-level assessments may reduce the level of accuracy possible for tree-level measurements. Important considerations in validating individual tree measurements include accounting for measurement error in validation data and assessing the accuracy of point cloud registration (Hopkinson *et al*., 2004; Thies *et al*., 2004).

The terrain and canopy height models described were not directly compared to a known standard, but they do compare heuristically to applications of airborne lidar. Typical applications of airborne lidar over vegetated surfaces have used interpolation to create digital elevation models using nominal cell sizes ranging from 0.5 m × 0.5 m to 5 m × 5 m (Popescu *et al*., 2002; MacMillan *et al*., 2003; Tenenbaum *et al*., 2006). Using a ground-based scanning system Schmid *et al*. (2004) were able to model micro-topography using 5 mm and 10 mm cell sizes on a 5 m × 7 m plot. For a forested plot (30 m × 30 m), Aschoff *et al*. (2004) created terrain models using 0.5 m × 0.5 m cells using a ground-based scanning laser. Here agreement between the leaf-off and leaf-on models (Table 2 and Figure 7), as well as their correspondence with GPS measurements (Figure 6), indicated that accurate surface models could be created with ground-based laser scanning. Terrain and canopy surface models from ground-based systems provided data at scales and resolutions that can be complimentary to airborne-derived models. Such models may be useful for co-registering and comparing airborne and ground-based data.

One objective of this research was to examine the differences between laser-scanner data obtained during leaf-off and leaf-on conditions and those comparisons support the application of ground-based scanning for multi-temporal observation. The correspondence between the leaf-off and leaf-on datasets allowed for direct evaluation of measured differences between the two conditions (Figure 4, Plate 1, and Plate 2). Recently, research has explored the application of airborne lidar for determining forest and individual tree growth using multi-temporal measurements (St-Onge and Vepakomma, 2004; Naesset and Gobakken, 2005). The use of ground-based laser scanning should be useful for evaluating growth and change in forest canopies, canopy gaps, understory development, and fuel loading, as well as damage from insects, disease, and storms. The registration of ground-based data sets across time, although not explored here, should prove useful for multi-temporal change detection in monitoring permanent sample plots.

The 3D spatial variability of canopy structure was exhibited in a number of our results. Ground-based laser scanning provided an efficient means to characterize this variability and relate it to differential tree growth and forest productivity. The future implementation of ground-based laser scanning for canopy characterization will depend on increased sophistication and automation of methods for registering, segmenting, and analyzing data, as well as complete validation of scanner-derived estimates.

References

Aber, J.D., and C.A. Federer, 1992. A generalized, lumped-parameter model of photosynthesis, evapotranspiration and net primary production in temperate and boreal forest ecosystems, *Oecologia*, 92(4):463–474.

Aschoff, T., M. Thies, and H. Spiecker, 2004. Describing forest stands using terrestrial laser-scanning, *Proceedings of the XXth ISPRS Congress: Geo-Imagery Bridging Continents*, 12–23 July, Istanbul, Turkey, pp. 237–241.

Avery, T.E., and H.E. Burkhart, 2002. *Forest Measurements*, Fifth edition, McGraw Hill, Boston, Massachusetts, 456 p.

Axelsson, P.E., 1999. Processing of laser scanner data-algorithms and applications, *ISPRS Journal of Photogrammetry and Remote Sensing*, 54(2–3):138–147.

Besl, P.J., and N.D. McKay, 1992. A method for registration of 3-D shapes, *IEEE Transactions on Pattern Analysis and Machine Intelligence*, 14(2):239–256.

Bolstad, P.V., J.M. Vose, and S.G. McNulty, 2001. Forest productivity, leaf area, and terrain in southern Appalachian deciduous forests, *Forest Science*, 47(3):419–427.

Bréda, N.J.J., 2003. Ground-based measurements of leaf area index: A review of methods, instruments and current controversies, *Journal of Experimental Botany*, 54(392):2403–2417.

Brunner, A., 1998. A light model for spatially explicit forest stand models, *Forest Ecology and Management*, 107(1–3):19–46.

Brunner, A., and G. Nigh, 2000. Light absorption and bole volume growth of individual Douglas-fir trees, *Tree Physiology*, 20(5–6): 323–332.

Canham, C.D., J.S. Denslow, W.J. Platt, J.R. Runkle, T.A. Spies, and P.S. White, 1990. Light regimes beneath closed canopies and tree-fall gaps in temperate and tropical forests, *Canadian Journal of Forest Research*, 20(5):620–631.

Canham, C.D., A.C. Finzi, S.W. Pacala, and D.H. Burbank, 1994. Causes and consequences of resource heterogeneity in forests – Interspecific variation in light transmission by canopy trees, *Canadian Journal of Forest Research*, 24(2):337–349.

Chasmer, L., C. Hopkinson, and P. Treitz, 2004. Assessing the 3D-frequency distribution of airborne and ground-based LIDAR data for red pine and mixed deciduous forest plots, *Proceedings of the ISPRS Working Group VIII/2: Laser-Scanners for Forest and Landscape Assessment*, 03–06 October, Freiburg, Germany, pp. 66–70.

Chazdon, R.L., and R.W. Pearcy, 1991. The importance of sunflecks for forest understory plants – Photosynthetic machinery appears adapted to brief, unpredictable periods of radiation, *Bioscience*, 41(11):760–766.

Chen, J.M., T.A. Black, and R.S. Adams, 1991. Evaluation of hemispherical photography for determining plant-area index and geometry of a forest stand, *Agricultural and Forest Meteorology*, 56(1–2):129–143.

Comeau, P.G., F. Gendron, and T. Letchford, 1998. A comparison of several methods for estimating light under a paper birch mixedwood stand, *Canadian Journal of Forest Research*, 28(12): 1843–1850.

Dai, X.B., 1996. Influence of light conditions in canopy gaps on forest regeneration: A new gap light index and its application in a boreal forest in east-central Sweden, *Forest Ecology and Management*, 84(1–3):187–197.

Drake, J.B., R.O. Dubayah, R.G. Knox, D.B. Clark, and J.B. Blair, 2002. Sensitivity of large-footprint lidar to canopy structure and biomass in a neotropical rainforest, *Remote Sensing of Environment*, 81(2–3):378–392.

Fitzgibbon, A.W., D.W. Eggert, and R.B. Fisher, 1997. High level CAD model acquisition from range images, *Computer-Aided Design*, 29(4):321–330.

Ford, E.D., and P.J. Newbould, 1971. The leaf canopy of a coppiced deciduous woodland: I. Development and structure, *Journal of Ecology*, 59:843–862.

Gendron, F., C. Messier, and P.G. Comeau, 1998. Comparison of various methods for estimating the mean growing season percent photosynthetic photon flux density in forests, *Agricultural and Forest Meteorology*, 92(1):55–70.

Gorte, B., and N. Pfeifer, 2004. Structuring laser-scanned trees using 3D mathematical morphology, *Proceedings of the XXth ISPRS Congress: Geo-Imagery Bridging Continents*, 12–23 July, Istanbul, Turkey, pp. 929–933.

Gorte, B., and D. Winterhalder, 2004. Reconstruction of laser-scanned trees using filter operations in the 3D raster domain, *Proceedings of the ISPRS Working Group VIII/2: Laser-Scanners for Forest and Landscape Assessment*, 03–06 October, Freiburg, Germany, pp. 39–44.

Gratzer, G., C. Canham, U. Dieckmann, A. Fischer, Y. Iwasa, R. Law, M.J. Lexer, H. Sandmann, T.A. Spies, B.E. Splechtna, and J. Szwagrzyk, 2004. Spatio-temporal development of forests – Current trends in field methods and models, *Oikos*, 107(1): 3–15.

Harding, D.J., M.A. Lefsky, G.G. Parker, and J.B. Blair, 2001. Laser altimeter canopy height profiles – Methods and validation for closed-canopy, broadleaf forests, *Remote Sensing of Environment*, 76(3):283–297.

Henning, J.G., 2005. *Modeling Forest Canopy Distribution from Ground-based Laser Scanner Data*, Ph.D. Dissertation, Virginia Polytechnic Institute and State University, Blacksburg, Virginia.

Henning, J.G., and P.J. Radtke, 2006. Detailed stem measurements of standing trees from ground-based scanning lidar, *Forest Science*, 52:67–80.

Hetzel, G., B. Leibe, P. Levi, and B. Schiele, 2001. 3D object recognition from range images using local feature histograms, *Proceedings of the 2001 IEEE Computer Society Conference on Computer Vision and Pattern Recognition*, 08–14 December, Kauai, Hawaii, IEEE Computer Society, Los Alamitos, California, pp. 394–399.

Hopkinson, C., L. Chasmer, C. Young-Pow, and P. Treitz, 2004. Assessing forest metrics with a ground-based scanning lidar, *Canadian Journal of Forest Research*, 34:573–583.

Kussner, R., and R. Mosandl, 2000. Comparison of direct and indirect estimation of leaf area index in mature Norway spruce stands of eastern Germany, *Canadian Journal of Forest Research*, 30(3):440–447.

Lefsky, M.A., W.B. Cohen, S.A. Acker, G.G. Parker, T.A. Spies, and D. Harding, 1999. Lidar remote sensing of the canopy structure and biophysical properties of Douglas-fir western hemlock forests, *Remote Sensing of Environment*, 70(3):339–361.

Lovell, J.L., D.L.B. Jupp, D.S. Culvenor, and N.C. Coops, 2003. Using airborne and ground-based ranging lidar to measure canopy structure in Australian forests, *Canadian Journal of Remote Sensing*, 29(5):607–622.

MacArthur, R.H., and H.S. Horn, 1969. Foliage profile by vertical measurements, *Ecology*, 5:802–804.

MacFarlane, D.W., E.J. Green, A. Brunner, and R.L. Amateis, 2003. Modeling loblolly pine canopy dynamics for a light capture model, *Forest Ecology and Management*, 173(1–3):145–168.

MacFarlane, D.W., E.J. Green, A. Brunner, and H.E. Burkhart, 2002. Predicting survival and growth rates for individual loblolly pine trees from light capture estimates, *Canadian Journal of Forest Research*, 32(11):1970–1983.

MacMillan, R.A., T.C. Martin, T.J. Earle, and D.H. McNabb, 2003. Automated analysis and classification of landforms using high-resolution digital elevation data: Applications and issues, *Canadian Journal of Remote Sensing*, 29(5):592–606.

Martin, J.G., B.D. Kloeppel, T.L. Schaefer, D.L. Kimbler, and S.G. McNulty, 1998. Aboveground biomass and nitrogen allocation of ten deciduous southern Appalachian tree species, *Canadian Journal of Forest Research*, 28(11):1648–1659.

Naesset, E., and T. Gobakken, 2005. Estimating forest growth using canopy metrics derived from airborne laser scanner data, *Remote Sensing of Environment*, 96(3–4):453–465.

Nelson, R., R. Swift, and W. Krabill, 1988. Using airborne lasers to estimate forest canopy and stand characteristics, *Journal of Forestry*, 86(10):31–38.

Parent, S., and C. Messier, 1996. A simple and efficient method to estimate microsite light availability under a forest canopy, *Canadian Journal of Forest Research*, 26(1):151–154.

Parker, G.G., D.J. Harding, and M.L. Berger, 2004. A portable LIDAR system for rapid determination of forest canopy structure, *Journal of Applied Ecology*, 41(4):755–767.

Pfeifer, N., B. Gorte, and D. Winterhalder, 2004. Automatic reconstruction of single trees from terrestrial laser scanner data, *Proceedings of the XXth ISPRS Congress: Geo-Imagery Bridging Continents*, 12–23 July, Istanbul, Turkey, pp. 114–119.

Popescu, S.C., R.H. Wynne, and R.F. Nelson, 2002. Estimating plot-level tree heights with lidar: Local filtering with a canopy-height based variable window size, *Computers and Electronics in Agriculture*, 37(1–3):71–95.

Radtke, P.J., and P.V. Bolstad, 2001. Laser point-quadrat sampling for estimating foliage-height profiles in broad-leaved forests, *Canadian Journal of Forest Research*, 31:410–418.

Rhoads, A.G., S.P. Hamburg, T.J. Fahey, T.G. Siccama, and R. Kobe, 2004. Comparing direct and indirect methods of assessing canopy structure in a northern hardwood forest, *Canadian Journal of Forest Research*, 34(3):584–591.

Schmid, T., H. Schack-Kirchner, and E. Hildebrand, 2004. A case study of terrestrial laser scanning in erosion research: calculation of roughness and volume balance at a logged forest site, *Proceedings of the ISPRS Working Group VIII/2: Laser-Scanners for Forest and Landscape Assessment*, 03–06 October, Freiburg, Germany, pp. 114–118.

St-Onge, B., and U. Vepakomma, 2004. Assessing forest gap dynamics and growth using multi-temporal laser-scanner data, *Proceedings of the ISPRS Working Group VIII/2: Laser-Scanners for Forest and Landscape Assessment*, 03–06 October, Freiburg, Germany, pp. 173–178.

Tanaka, T., H. Park, and S. Hattori, 2004. Measurement of forest canopy structure by a laser plane range-finding method improvement of radiative resolution and examples of its application, *Agricultural and Forest Meteorology*, 125(1–2): 129–142.

Tanaka, T., J. Yamaguchi, and Y. Takeda, 1998. Measurement of forest canopy structure with a laser plane range-finding method – Development of a measurement system and applications to real forests, *Agricultural and Forest Meteorology*, 91:149–160.

Tenenbaum, D.E., L.E. Band, S.T. Kenworthy, and C.L. Tague, 2006. Analysis of soil moisture patterns in forested and suburban catchments in Baltimore, Maryland, using high-resolution photogrammetric and LIDAR digital elevation datasets, *Hydrological Processes*, 20(2):219–240.

Thies, M., N. Pfeifer, D. Winterhalder, and B.G.H. Gorte, 2004. Three-dimensional reconstruction of stems for assessment of taper, sweep and lean based on laser scanning of standing trees, *Scandinavian Journal of Forest Research*, 19(6):571–581.

Thies, M., and H. Spiecker, 2004. Evaluation and future prospects of terrestrial laser scanning for standardized forest inventories, *Proceedings of the ISPRS Working Group VIII/2: Laser-Scanners for Forest and Landscape Assessment*, 03–06 October, Freiburg, Germany, pp. 192–197.

Tickle, P.K., A. Lee, R.M. Lucas, J. Austin, and C. Witte, 2006. Quantifying Australian forest floristics and structure using small footprint LiDAR and large scale aerial photography, *Forest Ecology and Management*, 223(1–3):379–394.

van Gardingen, P.R., G.E. Jackson, S. Hernandez-Daumas, G. Russell, and L. Sharp, 1999. Leaf area index estimates obtained for clumped canopies using hemispherical photography, *Agricultural and Forest Meteorology*, 94(3–4):243–257.

Warren Wilson, J., 1959. Analysis of the spatial distribution of foliage by two-dimensional point quadrats, *New Phytologist*, 58:92–101.

Warren Wilson, J., 1963. Estimation of foliage denseness and foliage angle by inclined point quadrats, *Australian Journal of Botany*, 11:95–105.

Watt, P.J., and D.N.M. Donoghue, 2005. Measuring forest structure with terrestrial laser scanning, *International Journal of Remote Sensing*, 26(7):1437–1446.

Zhilkin, P., and M.E. Alexander, 2000. 3D image registration using a fast noniterative algorithm, *Magnetic Resonance Imaging*, 18(9):1143–1150.

Zimble, D.A., D.L. Evans, G.C. Carlson, R.C. Parker, S.C. Grado, and P.D. Gerard, 2003. Characterizing vertical forest structure using small-footprint airborne lidar, *Remote Sensing of Environment*, 87(2–3):171–182.